Simultaneous Removal of Calconcarboxylic Acid, NH4+ and PO43? from Pharmaceutical Effluent Using Iron Oxide-Biochar Nanocomposite Loaded with Pseudomonas putida

Authors:

Saifeldin M. Siddeeg, Mohamed A. Tahoon, Faouzi Ben Rebah

Date Submitted: 2019-12-16

Keywords: calconcarboxylic acid, microorganisms, biochar, nanocomposites, industrial wastewater

Abstract:

In the current study, the Fe2O3/biochar nanocomposite was synthesized through a self-assembly method, followed by the immobilization of Pseudomonas putida (P. putida) on its surface to produce the P. putida/Fe2O3/biochar magnetic innovative nanocomposite. The synthesized nanocomposite was characterized using different techniques including X-ray diffraction, transmission electron microscopy (TEM), scanning electron microscopy (SEM), and Fourier-transform infrared spectroscopy (FT-IR). Then, the efficiencies of this material to remove calconcarboxylic acid (CCA) organic dye, ammonium ions (NH4+), and phosphate ions (PO43?) from industrial wastewater were analyzed. The removal rates of up to 82%, 95%, and 85% were achieved for CCA dye, PO43?, NH4+, respectively, by the synthesized composite. Interestingly, even after 5 cycles of reuse, the prepared nanocomposite remains efficient in the removal of pollutants. Therefore, the P. putida/Fe3O4/biochar composite was found to be an actual talented nanocomposite for industrial wastewater bioremediation.

Record Type: Published Article

Submitted To: LAPSE (Living Archive for Process Systems Engineering)

Citation (overall record, always the latest version):	LAPSE:2019.1604
Citation (this specific file, latest version):	LAPSE:2019.1604-1
Citation (this specific file, this version):	LAPSE:2019.1604-1v1

DOI of Published Version: https://doi.org/10.3390/pr7110800

processes

MDPI

Article

Simultaneous Removal of Calconcarboxylic Acid, NH_4^+ and PO_4^{3-} from Pharmaceutical Effluent Using Iron Oxide-Biochar Nanocomposite Loaded with *Pseudomonas putida*

Saifeldin M. Siddeeg [1,2], Mohamed A. Tahoon [1] and Faouzi Ben Rebah [1,3,*]

1 Department of Chemistry, College of Science, King Khalid University, P.O. Box 9004, Abha 61413, Kingdom of Saudi Arabia; saif.siddeeg@gmail.com (S.M.S.); tahooon_87@yahoo.com (M.A.T.)
2 Chemistry and Nuclear Physics Institute, Atomic Energy Commission, P.O. Box 3001, Khartoum 11111, Sudan
3 Higher Institute of Biotechnology of Sfax (ISBS), Sfax University, P.O. Box 263, Sfax 3000, Tunisia
* Correspondence: benrebahf@yahoo.fr

Received: 28 September 2019; Accepted: 23 October 2019; Published: 3 November 2019

Abstract: In the current study, the Fe_2O_3/biochar nanocomposite was synthesized through a self-assembly method, followed by the immobilization of *Pseudomonas putida* (*P. putida*) on its surface to produce the *P. putida*/Fe_2O_3/biochar magnetic innovative nanocomposite. The synthesized nanocomposite was characterized using different techniques including X-ray diffraction, transmission electron microscopy (TEM), scanning electron microscopy (SEM), and Fourier-transform infrared spectroscopy (FT-IR). Then, the efficiencies of this material to remove calconcarboxylic acid (CCA) organic dye, ammonium ions (NH_4^+), and phosphate ions (PO_4^{3-}) from industrial wastewater were analyzed. The removal rates of up to 82%, 95%, and 85% were achieved for CCA dye, PO_4^{3-}, NH_4^+, respectively, by the synthesized composite. Interestingly, even after 5 cycles of reuse, the prepared nanocomposite remains efficient in the removal of pollutants. Therefore, the *P. putida*/Fe_3O_4/biochar composite was found to be an actual talented nanocomposite for industrial wastewater bioremediation.

Keywords: industrial wastewater; nanocomposites; biochar; microorganisms; calconcarboxylic acid

1. Introduction

Calconcarboxylic acid (CCA), also known as 2-Hydroxy-1-(2-hydroxy-4-sulfo-1-naphthylazo)-3-naphthoic acid, is an important organic compound used in pharmaceutical industries as an indicator for Ca^{2+} determination in the presence of Mg^{2+} ions by titration against EDTA at pH 12 [1]. CCA has acute health effects such as irritation or damage of the human eye, skin inflammation, and lung damage in case of inhalation, while long-term exposure may lead to pneumoconiosis and bladder cancer. In addition, there are negative influences on the biotic environment components by azo dyes, such as the carcinogenic effect on living marine organisms and the inhibition of photosynthesis in plants [2]. Thus, azo dyes in industrial wastewater must be treated properly before it is released to the environment. Many efforts have been made to use microorganisms as a friendly process for wastewater treatment by degrading pollutants through their metabolism [3–8]. However, various factors such as cell recovery and slow biodegradation are likely to limit the application of the biological wastewater treatment process. In addition to CCA, PO_4^{3-} and NH_4^+ released into water bodies represent a real problem for human and environment as their high levels lead to eutrophication phenomenon resulting from high algae productivity [9]. Therefore, the efficient removal of PO_4^{3-} and NH_4^+ from

wastewater is essential to prevent water bloom and eutrophication. Recently, studies have been done to efficiently remove PO_4^{3-} and NH_4^+ from wastewater [10–13]. Pharmaceutical wastewater treatment faces difficult challenges due to the difficulty of treatment as this wastewater is a complex matrix containing various components like the CCA dye. Many researchers from all over the world have made efforts to treat real pharmaceutical wastewater samples [14–17]. To reduce effectively the pollutant concentration to an acceptable and safe rate, it is very important to look for an appropriate technique. Therefore, in the present study, nanotechnology and biodegradation were combined as a potential technique to remove CCA azo dye, PO_4^{3-}, and NH_4^+ from industrial wastewater. The combination is performed between Fe_3O_4 nanoparticles with biochar and *Pseudomonas putida* (*P. putida*) bacteria to benefit from the properties of each component. High reactivity, natural abundance, and magnetic recyclability are excellent features of iron oxide nanoparticles, allowing for their use in remediation processes [18,19]. However, all these advantages face the spontaneous aggregation of Fe_3O_4 nanoparticles in a solution that inhibits their function. Consequently, Fe_3O_4 nanoparticles were loaded over carriers (biochar) to prevent their aggregation. Biomass pyrolysis in the absence of oxygen leads to the production of carbon-rich biochar useful in different applications such as mitigated climate change, CO_2 removal [20–25], cathode materials in battery [26], soil fertility [27], and pollutant removal (organic compounds and heavy metals) [28–30] due to its porous properties, abundant functional groups, and alkaline nature. Each component of the *P. putida*/Fe_3O_4 nanoparticles/biochar nanocomposite has a function: Fe_3O_4 nanoparticles is for adsorption and magnetic separation, biochar is for adsorption, and *P. Putida* is for biodegradation. Thus, the Fe_3O_4 nanoparticles/biochar nanocomposite was prepared firstly and followed by the immobilization of *P. Putida* bacteria on the composite surface. The chemical characterization of the composite was performed as well as investigation into its ability to remove CCA, PO_4^{3-}, and NH_4^+ from pharmaceutical effluents.

2. Materials and Methods

2.1. Chemicals and Water Sample Collection

$FeSO_4$ was supplied from Sigma-Aldrich (St. Louis, Missouri, USA) while $FeCl_3$ was supplied from Xilong Scientific Co. (Shantou, China). Biochar was supplied from Biochar Now Co. (Berthoud, Colorado, USA). An ammonia aqueous solution (33%, v/v) was supplied from Al-Nasr Co. (Helwan, Egypt). All chemicals were used in the commercial form without any purification. Industrial wastewater samples were collected from the drainage of Mansoura Co. (Cairo, Egypt) for medical and pharmaceutical industries, Gamasa industrial region, Egypt.

2.2. Preparation of the Iron Oxide/Biochar Nanocomposite

Iron oxide (Fe_3O_4) nanoparticles were prepared by mixing $FeSO_4$ and $FeCl_3$ with a 1:2 molar ratio in the presence of an adequate quantity of an aqueous ammonium solution. Then, the mixture was stirred for 40 min under a nitrogen atmosphere. The formed nanoparticles were separated (using a magnet) and washed several times with distilled water. Then, 2 g of biochar was gridded and sieved through a 0.2 mm mesh. Fe_3O_4 nanoparticles were suspended in a 400 mL deionized water and the gridded biochar was added to the suspension and stirred for 5 h. Finally, the composite was separated with a magnet, washed several times with distilled water and kept to dry in the oven for 6 h at 85 °C. The resulted Fe_3O_4/biochar nanocomposite was characterized using many techniques including X-ray diffraction (XRD) from 10° to 70° of 2θ region using Rigaku MiniFlex 600 X-ray Diffractometer with the Cu Kα radiation (λ = 1.54051 Å). The scanning electron microscopy (SEM; Philips XL30 ESEM) was used to obtain SEM images of the prepared nanocomposite. For transmission electron microscopy (TEM) images, the nanocomposite was ground and suspended in water, and the supernatant was used for sample preparation. Additionally, Fourier-transform infrared (FT-IR) spectra of prepared materials were obtained using the Nicolet Magna FT-IR spectrometer from 400 cm^{-1} to 4000 cm^{-1}.

2.3. Bacteria Cultivation and Immobilization on the Iron Oxide/Biochar Nanocomposite

P. putida bacterial strain used in the biodegradation process were cultivated in a growth medium containing Na_2CO_3, agar, glucose (3%, w/v), KH_2PO_4, yeast extract, and $MgSO_4$ at a neutral pH value and 30 °C for 72 h. After growth, bacterial cells were collected and washed several times with distilled water. Then, the cells were suspended in water. In the 400 mL culture solution, 1 g of suspended cells was mixed with the nanocomposite of a similar weight on a shaker for 3 h to allow for the complete adsorption of the bacterial cell inside the pores of the nanocomposite. The immobilized composite was washed three times by distilled water to remove un-adsorbed cells after collection by a magnet from the solution. The obtained *P. putida*/Fe_3O_4 nanoparticles/biochar composite was used to remove CCA, PO_4^{3-}, and NH_4^+ from the industrial effluent.

2.4. Industrial Wastewater Content and Batch Study

The wastewater contents of CCA, NH_4^+, and PO_4^{3-} were determined using LC–MS/MS, a Nessler reagent colorimetric method, and a molybdenum blue spectrophotometer, respectively. The concentrations were found to be 2.5 mg/mL for CCA, 11.1 mg/mL for NH_4^+, and 3.4 mg/mL for PO_4^{3-}. Batch experiments were carried out in 250 mL flask at room temperature and pH 7. Wastewater-free agents were set as a control while 100 mL of wastewater were mixed with free bacterial cells (0.06 g wet weight as an immobilized amount), Fe_3O_4/biochar composite (0.12 g), and *P. putida*/Fe_3O_4/biochar composite (0.06 g bacterial cell wet weight and 0.06 g Fe_3O_4/biochar composite). Then, a magnet was used to take a sample from the suspension at different times of the experiment and passed through a Whatman Grade 42 filter paper (0.45 μm) before being analyzed for CCA, NH_4^+, and PO_4^{3-}. After each experiment, the composite separated by a magnet was gently washed with deionized and its reusability was tested. Each experiment was conducted in triplicate.

3. Results and Discussion

3.1. Characterization of the P. putida/Fe_3O_4/Biochar Composite

The prepared Fe_3O_4 nanoparticles, biochar, and Fe_3O_4/biochar nanocomposite were characterized using different techniques: TEM, SEM, FT-IR, and XRD. The SEM and TEM images are presented in Figure 1, in which the morphology of Fe_3O_4 nanoparticles is clear spherical with a 11 nm particle size. A rough and porous biochar surface is clearly shown in an SEM image (Figure 1d). This surface is excellent to allow for uniform dispersion of iron oxide nanoparticles and reduce the aggregation process of nanoparticles. XRD and FT-IR spectra of the biochar, Fe_3O_4 nanoparticles, and Fe_3O_4/biochar nanocomposite were presented in Figure 2a,b. In terms of the FT-IR spectra (Figure 2b), there is a match between the composite and biochar spectra, but the presence of the Fe–O band at 637 cm^{-1} (stretching vibration) indicates the presence of the iron oxide in the composite. According to XRD in Figure 2a, the crystalline structure is indicated due to the appearance of strong sharp bands in nanoparticles and nanocomposites. The peak matching between nanoparticles and nanocomposites indicates the adsorption of magnetic nanoparticles on the biochar surface.

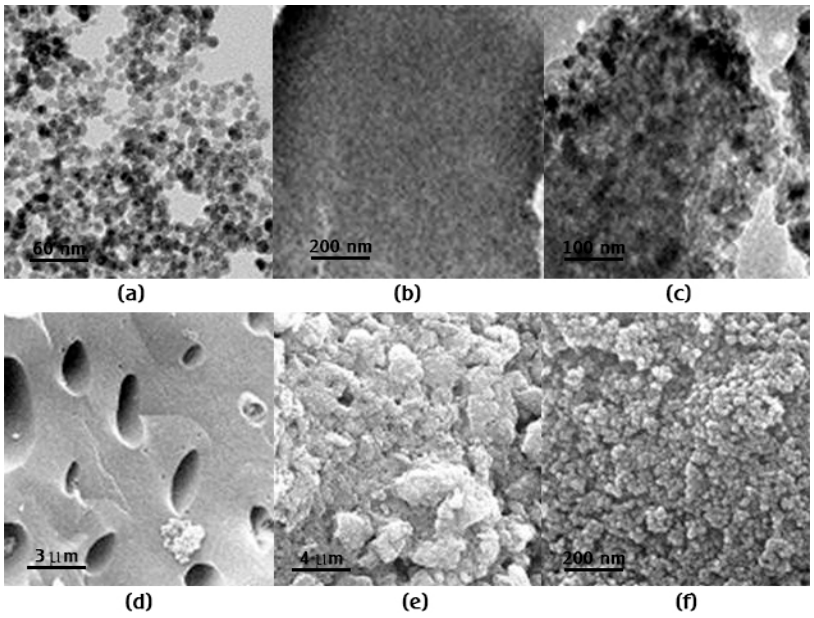

Figure 1. TEM images of Fe_3O_4 nanoparticles (**a**), biochar (**b**), and Fe_3O_4/biochar composite (**c**). SEM images of biochar (**d**), Fe_3O_4/biochar composite (**e**), and magnified SEM of Fe_3O_4/biochar composite (**f**).

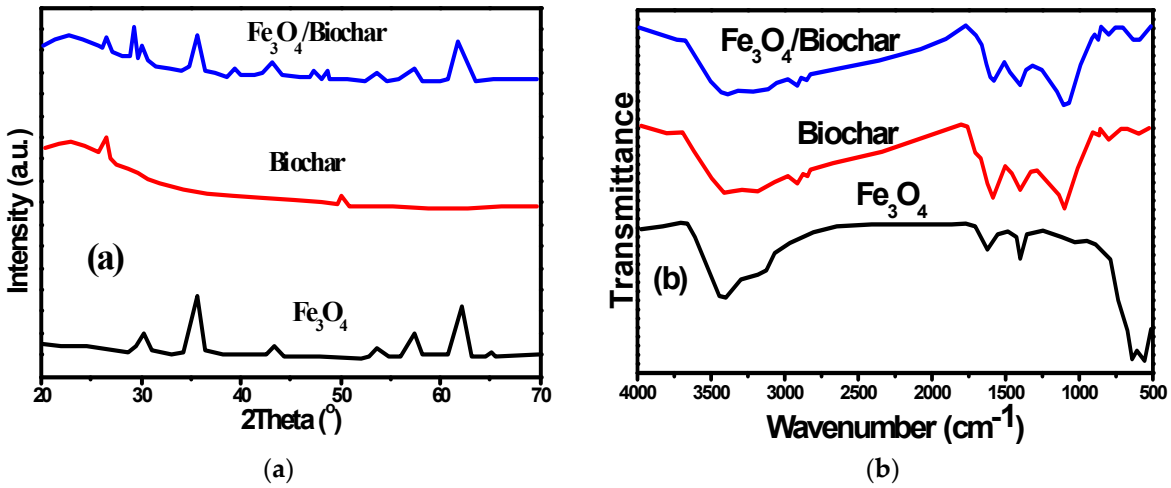

(**a**) (**b**)

Figure 2. XRD (**a**) and FT-IR (**b**) spectra of Fe_3O_4/biochar composite, biochar, and Fe_3O_4 nanoparticles.

3.2. Pollutants Removal

The prepared Fe_3O_4/biochar and *P. putida*/Fe_3O_4/biochar composites can be used separately as an efficient catalyst or sorbent for CCA, PO_4^{3-}, and NH_4^+ removal from pharmaceutical wastewater. For CCA, *P. putida* bacteria alone show effective removal of CCA organic dye as the bacteria can use organic materials in the phosphorylation process. The *P. putida* strain leads to a removal rate of CCA organic azo dye of 65% from the pharmaceutical wastewater after half an hour of incubation, as shown in Figure 3a. The CCA dye removal by the mean of Fe_2O_3/biochar nanocomposite reached 69% (Figure 3a) due to the high surface area resulting from its porous structure that enhances CCA adsorption on the composite surfaces. Moreover, its small energy gap (2.3 eV) [31] leads to the absorption of light that results in photo-degradation of the CCA organic dye, while the immobilization of *P. putida* on the surface of the composite leads to an achievement of 82% CCA removal from the industrial wastewater as indicated in Figure 3a, which is significantly greater than that reached by the bacteria alone and the nanocomposite. This improvement of CCA removal may have resulted from the triggering of the bacterial enzymatic activity, and growth and metabolism by iron ions of

the composite. The simulation of enzymatic activity was due to the presence of Fe–Fe bond inside the bacterial hydrogenase enzyme [32]. Therefore, the presence of iron nanoparticles enhances the enzymatic activity. Moreover, the growth and the bacterial metabolism were activated due to iron oxide nanoparticles that act as an extracellular acceptor of electrons [33]. Herein, the bacteria consume the organic pollutant CCA for its growth and metabolism.

For PO_4^{3-} and NH_4^+ removal from the industrial wastewater, *P. putida* bacteria alone show removal rates of 64% and 62% (Figure 3b,c), respectively. This result was expected as PO_4^{3-} and NH_4^+ are essentially utilized by bacteria for growth and metabolism during the phosphorylation process [34] and protein synthesis. The PO_4^{3-} removal by means of the Fe_2O_3/biochar nanocomposite reached 93% at the first 10 h which is attributed to the attraction between negatively charged phosphate ions and the oppositely charged iron oxides besides the formation of inner complexes by the replacement of phosphorus group with the hydroxyl group of magnetic oxide [35]. However, only 51% of NH_4^+ was removed by the Fe_2O_3/biochar nanocomposite as expected due to the repulsion between positively charged ammonium ions and ferric oxides. The higher removal rates of PO_4^{3-} (95%) and NH_4^+ (85%) were reached by means of the *P. putida*/Fe_2O_3/biochar nanocomposite. The obtained results for PO_4^{3-} and NH_4^+ removal rates are better than that for NH_4^+ removal with wetlands methods [36] and better than that for PO_4^{3-} removal in an activated sludge process [37].

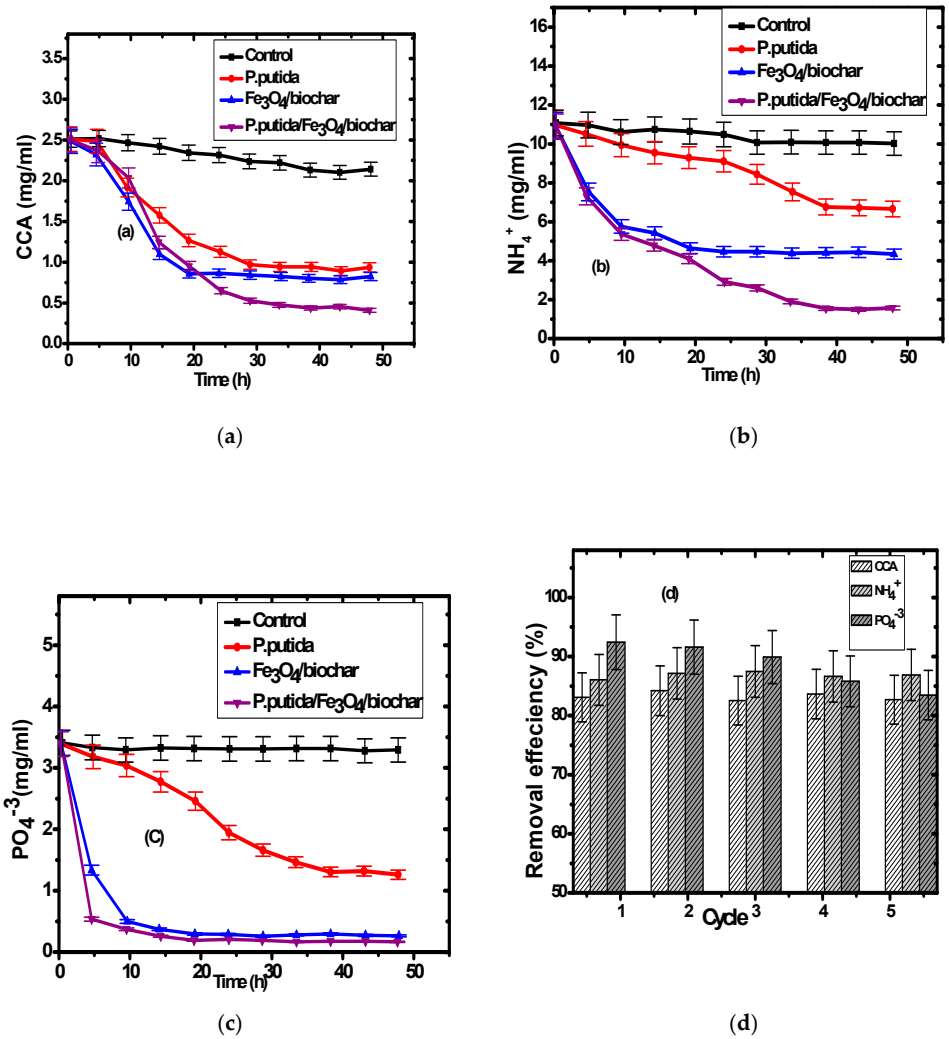

(**a**) (**b**)

(**c**) (**d**)

Figure 3. Removal of calconcarboxylic acid (CCA) (**a**), NH_4^+ (**b**), and PO_4^{3-} (**c**) by using *Pseudomonas putida* (*P. putida*), Fe_3O_4/biochar, and *P. putida*/Fe_3O_4/biochar composites; (**d**) five-cycle pollutant removals.

3.3. Composite Reusability for Wastewater Treatment

The recyclability of nanocomposite is a significant feature for optimal wastewater treatment. In this context, there must be two key issues—whether the recycled catalyst can be readily retrieved and whether it retains its operation. Both elements are excellent for the *P. putida*/iron oxide nanoparticles/biochar composite. Interestingly, the main advantage of this composite is that it can be easily recovered by a bar magnet taking advantage of Fe_3O_4 magnetism. The magnetic property of iron oxide nanoparticles are an exceptional physical feature, which independently helps to purify water by affecting the physical characteristics of water pollutants. Additionally, the prepared composite does not lose its activity to remove CCA, PO_4^{3-}, and NH_4^+ from the pharmaceutical wastewater even after five cycles, as shown in Figure 3d. After five cycles, the composite efficiency removals are 85%–87% for NH_4^+ and 84% for CCA, while it decreased to 87% for PO_4^{3-} in cycle five. Based on these results discussed above, the prepared composite is an appropriate agent for pharmaceutical wastewater bioremediation.

4. Conclusions

In the present research, the self-assembly technique was used to prepare iron oxide nanoparticles/biochar nanocomposites. Through a slight load, the oxide nanoparticles were well distributed on the surface of biochar. After the iron oxide nanoparticles/biochar nanocomposite preparation, *P. putida* strain cultivated in our laboratory were immobilized on the surface of the composite to finally produce the *P. putida*/Fe_2O_3/biochar nanocomposite efficiently for the removal of CCA organic dye, PO_4^{3-}, and NH_4^+ from pharmaceutical wastewater treatment. The magnetic feature of the prepared composite allows for its reuse in many cycles with high activity toward pollutants removal. However, more research is needed to explore other types of industrial wastewaters and to determine the optimal treatment factors (pH, temperature, dosage, etc.). Finally, the efficiency of this process should be studied at a large scale, in a real environment, and for wastewaters from various origins, followed by a techno-economic evaluation.

Author Contributions: Conceptualization, F.B.R., S.M.S., and M.A.T.; investigation, M.A.T. and S.M.S; data curation, F.B.R. and S.M.S.; writing of original draft preparation, M.A.T. and S.M.S.; writing of review and editing, M.A.T.; supervision, F.B.R.; project administration, F.B.R., S.M.S., and M.A.T.

Funding: This research was funded by the Deanship of Scientific Research at King Khalid University.

Acknowledgments: The authors extended their appreciation to the Deanship of Scientific Research at King Khalid University for funding this work through a research group project under grant number R.G.P2/45/40.

Conflicts of Interest: The authors declare that there are no conflicts of interest regarding the publication of this paper.

References

1. Patton, J.; Reeder, W. New indicator for titration of calcium with (ethylenedinitrilo) tetraacetate. *Anal. Chem.* **1956**, *28*, 1026–1028. [CrossRef]
2. Sahoo, M.K.; Sinha, B.; Sharan, R.N. Metal ion-catalyzed mineralization and biodetoxification studies of Calconcarboxylic acid in aqueous solution: Effect of–COOH group. *Desalin. Water Treat.* **2015**, *56*, 1955–1963. [CrossRef]
3. Shukla, V.Y.; Tipre, D.R.; Dave, S.R. Optimization of chromium (VI) detoxification by Pseudomonas aeruginosa and its application for treatment of industrial waste and contaminated soil. *Bioremediat. J.* **2014**, *18*, 128–135. [CrossRef]
4. Vassilev, N.; Fenice, M.; Federici, F.; Azcon, R. Olive mill waster water treatment by immobilized cells of Aspergillus niger and its enrichment with soluble phosphate. *Process Biochem.* **1997**, *32*, 617–620. [CrossRef]
5. Liu, B.-F.; Jin, Y.-R.; Cui, Q.-F.; Xie, G.-J.; Wu, Y.-N.; Ren, N.-Q. Photo-fermentation hydrogen production by Rhodopseudomonas sp. nov. strain A7 isolated from the sludge in a bioreactor. *Int. J. Hydrog. Energy* **2015**, *40*, 8661–8668. [CrossRef]

6. Nagadomi, H.; Kitamura, T.; Watanabe, M.; Sasaki, K. Simultaneous removal of chemical oxygen demand (COD), phosphate, nitrate and H_2S in the synthetic sewage wastewater using porous ceramic immobilized photosynthetic bacteria. *Biotechnol. Lett.* **2000**, *22*, 1369–1374. [CrossRef]
7. Lu, H.; Zhang, G.; Dai, X.; He, C. Photosynthetic bacteria treatment of synthetic soybean wastewater: Direct degradation of macromolecules. *Bioresour. Technol.* **2010**, *101*, 7672–7674. [CrossRef]
8. Idi, A.; Nor, M.H.M.; Wahab, M.F.A.; Ibrahim, Z. Photosynthetic bacteria: An eco-friendly and cheap tool for bioremediation. *Rev. Environ. Sci. Bio/Technol.* **2015**, *14*, 271–285. [CrossRef]
9. Heisler, J.; Glibert, P.M.; Burkholder, J.M.; Anderson, D.; Cochlan, W.; Dennison, W.C.; Dortch, Q.; Gobler, C.J.; Heil, C.A.; Humphries, E. Eutrophication and harmful algal blooms: A scientific consensus. *Harmful Algae* **2008**, *8*, 3–13. [CrossRef]
10. Barca, C.; Gérente, C.; Meyer, D.; Chazarenc, F.; Andrès, Y. Phosphate removal from synthetic and real wastewater using steel slags produced in Europe. *Water Res.* **2012**, *46*, 2376–2384. [CrossRef]
11. Kim, J.Y.; Balathanigaimani, M.; Moon, H. Adsorptive removal of nitrate and phosphate using MCM-48, SBA-15, chitosan, and volcanic pumice. *Water Air Soil Pollut.* **2015**, *226*, 431. [CrossRef]
12. Mazloomi, F.; Jalali, M. Ammonium removal from aqueous solutions by natural Iranian zeolite in the presence of organic acids, cations and anions. *J. Environ. Chem. Eng.* **2016**, *4*, 240–249. [CrossRef]
13. Zhang, T.; Li, Q.; Ding, L.; Ren, H.; Xu, K.; Wu, Y.; Sheng, D. Modeling assessment for ammonium nitrogen recovery from wastewater by chemical precipitation. *J. Environ. Sci.* **2011**, *23*, 881–890. [CrossRef]
14. Lucas, D.; Barceló, D.; Rodriguez-Mozaz, S. Removal of pharmaceuticals from wastewater by fungal treatment and reduction of hazard quotients. *Sci. Total Environ.* **2016**, *571*, 909–915. [CrossRef] [PubMed]
15. Shi, X.; Leong, K.Y.; Ng, H.Y. Anaerobic treatment of pharmaceutical wastewater: A critical review. *Bioresour. Technol.* **2017**, *245*, 1238–1244. [CrossRef] [PubMed]
16. Sarkar, S.; Bhattacharjee, C.; Sarkar, S. Studies on the performance of annular photo reactor (APR) for pharmaceutical wastewater treatment. *J. Water Process Eng.* **2017**, *19*, 26–34. [CrossRef]
17. Zhan, J.; Li, Z.; Yu, G.; Pan, X.; Wang, J.; Zhu, W.; Han, X.; Wang, Y. Enhanced treatment of pharmaceutical wastewater by combining three-dimensional electrochemical process with ozonation to in situ regenerate granular activated carbon particle electrodes. *Sep. Purif. Technol.* **2019**, *208*, 12–18. [CrossRef]
18. Kataria, N.; Garg, V. Green synthesis of Fe_3O_4 nanoparticles loaded sawdust carbon for cadmium (II) removal from water: Regeneration and mechanism. *Chemosphere* **2018**, *208*, 818–828. [CrossRef]
19. Wu, J.; Huang, D.; Liu, X.; Meng, J.; Tang, C.; Xu, J. Remediation of As (III) and Cd (II) co-contamination and its mechanism in aqueous systems by a novel calcium-based magnetic biochar. *J. Hazard. Mater.* **2018**, *348*, 10–19. [CrossRef]
20. Lehmann, J.; Joseph, S. *Biochar for Environmental Management: Science, Technology and Implementation*; Routledge: Abingdon-on-Thames, UK, 2015.
21. Dominic Woolf, D.; Amonette, J.E.; Street-Perrott, F.A.; Lehmann, J.; Joseph, S. Sustainable biochar to mitigate global climate change. *Nat. Commun.* **2010**, *1*, 56. [CrossRef]
22. Van Zwieten, L.; Kimber, S.; Morris, S.; Chan, K.Y.; Downie, A.; Rust, J.; Joseph, S.; Cowie, A. Effects of biochar from slow pyrolysis of papermill waste on agronomic performance and soil fertility. *Plant Soil* **2010**, *327*, 235–246. [CrossRef]
23. Ahmad, M.; Rajapaksha, A.U.; Lim, J.E.; Zhang, M.; Bolan, N.; Mohan, D.; Vithanage, M.; Lee, S.S.; Ok, Y.S. Biochar as a sorbent for contaminant management in soil and water: A review. *Chemosphere* **2014**, *99*, 203. [CrossRef] [PubMed]
24. Sujana, P. The application of biochar to screen printing liquid waste polluted land, its effect in soil, mustard greens to heavy metals (Fe, Cr). *RJTA* **2018**, *22*, 224–234. [CrossRef]
25. Sarpong, K.A.; Salazar, A.; Ortega, A.; Telles, K.; Djaman, K.; O'Neill, M.K.; Valles-Rosales, D.J.; Brewer, C.E. Pyrolysis of Wood Excelsior Residues for Biochar and Renewable Energy Production. In Proceedings of the 2018 ASABE Annual International Meeting: American Society of Agricultural and Biological Engineers, Detroit, MI, USA, 29 July–1 August 2018.
26. Chen, Z.-H.; Du, X.L.; He, J.B.; Li, F.; Wang, H.; Li, Y.L.; Li, B.; Xin, S. Porous coconut shell carbon offering high retention and deep lithiation of sulfur for lithium–sulfur batteries. *ACS Appl. Mater. Interfaces* **2017**, *9*, 33855–33862. [CrossRef]

27. El-Naggar, A.; Lee, S.S.; Awad, Y.M.; Yang, X.; Ryu, C.; Rizwan, M.; Ringklebe, J.; Tsang, D.C.W.; Ok, Y.S. Influence of soil properties and feedstocks on biochar potential for carbon mineralization and improvement of infertile soils. *Geoderma* **2018**, *332*, 100–108. [CrossRef]
28. Lin, Y.; Munroe, P.; Joseph, S.; Henderson, R.; Ziolkowski, A. Water extractable organic carbon in untreated and chemical treated biochars. *Chemosphere* **2012**, *87*, 151–157. [CrossRef]
29. Qin, H.Z.; Liu, Y.Y.; Li, L.Q.; Pan, G.X.; Zhang, X.H.; Zheng, J.W. Adsorption of cadmium solution by biochar from household biowaste. *J. Ecol. Rural. Environ.* **2012**, *28*, 181–186.
30. Xu, T.; Lou, L.; Luo, L.; Cao, R.; Duan, D.; Chen, Y. Effect of bamboo biochar on pentachlorophenol leachability and bioavailability in agricultural soil. *Sci. Total Environ.* **2012**, *414*, 727–731. [CrossRef]
31. Akhavan, O.; Azimirad, R. Photocatalytic property of Fe_2O_3 nanograin chains coated by TiO_2 nanolayer in visible light irradiation. *Appl. Catal. A Gen.* **2009**, *369*, 77–82. [CrossRef]
32. Khusnutdinova, A.N.; Ovchenkova, E.P.; Khristova, A.P.; Laurinavichene, T.V.; Shastik, E.S.; Liu, J.; Tsygankov, A.A. New tolerant strains of purple nonsulfur bacteria for hydrogen production in a two-stage integrated system. *Int. J. Hydrog. Energy* **2012**, *37*, 8820–8827. [CrossRef]
33. Kato, S.; Hashimoto, K.; Watanabe, K. Methanogenesis facilitated by electric syntrophy via (semi) conductive iron-oxide minerals. *Environ. Microbiol.* **2012**, *14*, 1646–1654. [CrossRef] [PubMed]
34. Wang, X.; Cheng, X.; Sun, D.; Ren, Y.; Xu, G. Simultaneous nutrient and carbon removal from azo dye wastewater using a photorotating biological contactor reactor. *J. Chem. Technol. Biotechnol.* **2014**, *89*, 1545–1552. [CrossRef]
35. Chen, J.; Yan, L.G.; Yu, H.Q.; Li, S.; Qin, L.L.; Liu, G.Q.; Li, Y.F.; Du, B. Efficient removal of phosphate by facile prepared magnetic diatomite and illite clay from aqueous solution. *J. Environ. Chem. Eng.* **2016**, *287*, 162–172. [CrossRef]
36. Wang, W.; Ding, Y.; Wang, Y.; Song, X.; Ambrose, R.F.; Ullman, J.L.; Winfrey, B.K.; Wang, J.; Gong, J. Treatment of rich ammonia nitrogen wastewater with polyvinyl alcohol immobilized nitrifier biofortified constructed wetlands. *Ecol. Eng.* **2016**, *94*, 7–11. [CrossRef]
37. Eldyasti, A.; Andalib, M.; Hafez, H.; Nakhla, G.; Zhu, J. Comparative modeling of biological nutrient removal from landfill leachate using a circulating fluidized bed bioreactor (CFBBR). *J. Hazard. Mater.* **2011**, *187*, 140–149. [CrossRef]